JOURNAL OF AIRCRAFT
Vol. 32, No. 3, May–June 1995

Correlation of Unsteady Pressure and Inflow Velocity Fields of a Pitching Rotor Blade

Mihir K. Lal,* S. G. Liou,* G. A. Pierce,† and N. M. Komerath‡
Georgia Institute of Technology, Atlanta, Georgia 30332

Predictions from four different analytical methods are compared with measurements of unsteady inflow velocity and surface pressure distributions on a pitching rotor blade in hover. The test case is a stiff two-bladed teetering rotor constructed from full-scale tail rotor blades, subjected to *n*/rev simple harmonic pitch oscillations under incompressible flow conditions. The chordwise distributions of unsteady pressure at three radial locations on the blade are compared with Theodorsen's and Loewy's two-dimensional incompressible unsteady aerodynamic theories and with Kaladi's pulsating doublet distribution method. Inflow velocity is predicted successfully using Peters' modal theory for steady as well as dynamic pitch conditions. The effect of dynamic inflow on rotor unsteady surface pressure is studied. At inboard radial locations, Loewy's two-dimensional theory for even harmonics of forcing frequency and Theodorsen's two-dimensional theory for odd harmonics provide efficient and reliable predictions of unsteady blade surface pressure. At outboard radial locations, panel or modal methods have to be used to predict amplitude and phase of unsteady pressure. Tip effects, mean pitch angle effects, and effects of rotation have been demonstrated.

Nomenclature

b	=	number of blades
$C(k)$	=	Theodorsen's lift deficiency function, $F + iG$
$C'(k)$	=	modified lift deficiency function for the rotor, $F' + iG'$
C_p	=	pressure coefficient, $2(p - p_\infty)/\rho\Omega^2 r^2 = C_{p_0} + C'_p$
C'_p	=	perturbation pressure coefficient
C_{p_0}	=	mean or nominal pressure coefficient
c	=	blade chord, 298 mm
h	=	nondimensional spacing between successive rows of vorticity, $\pi\nu/(cb\Omega)$
k	=	reduced frequency based on blade semi-chord, $c\omega/(2r\Omega) = nc/(2r)$
n	=	harmonics of forcing frequency, ω/Ω
q_i	=	ith component of perturbation velocity, nondimensionalized using ΩR
R	=	rotor radius, 1.295 m
r	=	radial location of blade section
U	=	local freestream velocity at the blade section, Ωr
$W(kh, n)$	=	wake weighting function
$w(x^*)$	=	normal wash at x^*
x	=	chordwise coordinate
x^*	=	nondimensional chordwise coordinate, $(=2x/c)$, with origin at midchord
z	=	coordinate along the axis of the rotor
z^*	=	nondimensional displacement of surface
$\Delta C'_p$	=	lifting perturbation pressure coefficient, $(C'_p)_{\text{lower}} - (C'_p)_{\text{upper}}$
θ	=	blade pitch angle, $\theta_0 + \theta'$
θ'	=	perturbation in pitch angle
θ_0	=	mean pitch angle
ν	=	steady inflow velocity
ξ	=	nondimensional coordinate along freestream direction, positive upstream
ξ^*	=	nondimensional dummy variable for integration
ρ	=	air density
Φ^A	=	pressure coefficient due to acceleration
Φ^V	=	pressure coefficient due to momentum flux
ψ	=	rotor azimuth angle
Ω	=	rotor speed
ω	=	forcing frequency

Presented as Paper 93-3082 at the AIAA 24th Fluid Dynamics Conference, Orlando, FL, July 6–9, 1993; received Dec. 2, 1993; revision received Sept. 8, 1994; accepted for publication Sept. 15, 1994.

*Postdoctoral Fellow, School of Aerospace Engineering. Member AIAA.
†Professor and Associate Director, School of Aerospace Engineering. Member AIAA.
‡Professor, School of Aerospace Engineering. Associate Fellow AIAA.

Introduction

THE primary uncertainty in analytical models for rotor blade aeroelastic phenomena is associated with the unsteady aerodynamics of the rotor. Unsteady aerodynamic loads on fixed wings for combined pitch and translation oscillations have been studied extensively by many researchers, but much remains unknown about similar loads on rotor blades. In addition to the effects of rotation, the rotor blade airloads are greatly affected by the very complex wake vortex structure. When the pitch changes rapidly, several complications arise. At large pitch angles, dynamic flow separation becomes a major issue, of interest in predicting blade characteristics on the retreating side of a rotor in forward flight. We avoid this regime in this article, and focus instead on the low-pitch, small-amplitude oscillation regime. Here, the unsteady boundary layer, the wake, and the shed vorticity all affect the blade loads, and both the magnitude and the phase of these effects must be considered to predict aeroelastic phenomena. Obviously, this is a regime where linearized analyses using quasisteady blade section data may be expected to be of value in developing aerodynamic models that can be computed efficiently enough to be coupled with structural dynamic analyses. Such approaches have been used for many years, but interest in this area has remained intense because of the extreme importance of blade dynamics and of blade aerodynamics in the prediction of dynamic blade loads. Development of theoretical models continues to be of interest, especially as results from comprehensive rotorcraft prediction codes en-

Table 1 Test conditions and associated parameters at 0.70*R*

$n = \omega/\Omega$ $k = nc/2r$	θ_0, deg	F	G	$h = 2\pi\nu/bQ\Omega$	$W(kh, n)$	F'	G'
5/rev $k = 0.82073$	4	0.552276	−0.114613	1.010883	−0.303717	0.747955	−0.067920
4/rev $k = 0.65658$	4	0.570367	−0.131170	1.010883	1.061550	0.328494	−0.184461
3/rev $k = 0.49444$	4	0.599696	−0.151755	1.010883	−0.378059	0.815340	−0.222282
2/rev $k = 0.32829$	4	0.651994	−0.175417	1.010883	2.540888	0.266966	−0.114582
4/rev $k = 0.65658$	2	—	—	0.566078	2.221408	0.246357	−0.220991
	6	—	—	1.389592	0.671029	0.382376	−0.165947
	8	—	—	1.725069	0.475313	0.420105	−0.155355
	10	—	—	2.029421	0.358366	0.447746	−0.148783

able comparison with rotorcraft flight test data and generate controversy over the sources of uncertainty. It has not been possible in the past to perform direct comparisons of the performance of these models against detailed experimental data on a rotor operating under controlled excitation. This article describes the results of such a comparison against detailed measurements of pressure and velocity fields for a rotor that is large enough to represent full-scale rotorcraft problems.

The prior work summarized below is that directly related to the low-amplitude, low-speed rotor blade pitching problem of interest here. Satyanarayana and Davis[1] studied the unsteady loading near the trailing edge of an oscillating wing for reduced frequencies from 0.5 to 1.2. The measured loading near the trailing edge differed from predictions using unsteady, incompressible, small-disturbance theory. This evidence of a violation of the Kutta condition increased with reduced frequency for $k > 0.8$. Ardonceau[2] measured unsteady surface pressure on a rectangular wing for $k \leq 1.5$ and compared results with the computations of Ref. 3. The airfoil was represented by source/sink segments and a constant vortex density over the whole surface. The singularity strengths were obtained from the system of linear equations to satisfy zero normal relative velocity at each segment center. The Kutta condition was zero differential loading at the trailing edge. Partial linearization was used for the wake. At low k, the amplitude agreed well, but phase disagreed near the trailing edge. At high k, the phase agreed well, but amplitude differed slightly. Commerford and Carta[4] measured the unsteady pressure on an airfoil due to vortex shedding from an upstream cylinder at $k = 3.9$. Lorber and Covert[5] measured airfoil unsteady pressure induced by an elliptic cylinder rotating downstream for $k \leq 6.4$, and compared with predictions from thin airfoil theory with measured unsteady cylinder upwash. A phase discrepancy appeared near the trailing edge.

Clearly, the prediction of the complex unsteady surface pressure and the unsteady inflow velocity, involving both amplitude and phase, are major issues. There are several added rotor effects. They include the varying freestream velocity along the radius (span), the proximity of several turns of concentrated tip vortices and layers of vorticity in the rotor wake, the differences in the periodicity of the phenomena based on the number of blades (whether odd or even), the finite-span effects including those of the circulation distribution on the rotor (very different from that of a fixed wing), and the centrifugal effects of rotation. In this article, the measurements of inflow velocity and unsteady pressure on a two-bladed rotor in hover, described in Refs. 6 and 7, respectively, are correlated with four different analytical formulations. Analytical results on dynamic inflow velocity have been taken from Ref. 8, computed using Peters' modal method. Analytical results on chordwise pressure distributions have been obtained from Kaladi's panel method described in Ref. 9. Also, Theodorsen's[10] and Loewy's[11] two-dimensional unsteady aerodynamic theories, which are well-known classical methods, have been used to correlate the measured unsteady pressure. The unsteadiness is driven by dynamic pitch excitation of the stiff rotor blades. The facility, calibration, kinematic relations, and measurement techniques are described in Refs. 6 and 7. Reference 6 describes previous work on measuring rotor velocity fields as well as in modeling dynamics. It goes on to describe measurements of dynamic inflow velocity at two axial locations slightly upstream of the rotor tip path plane and uses flow visualization to document the tip wake trajectory in the immediate vicinity of the rotor. Reference 7 describes the problem of measuring unsteady blade surface pressure on pitching rotor blades, their solution, and the results of those measurements.

Summary of Experiments

Part I: Inflow Velocity

The experiments were conducted in the Aeroelastic Rotor Test Chamber at Georgia Institute of Technology.[6] The two-bladed Bell 212 teetering tail rotor has a diameter of 2.58 m and blade chord of 0.292 m. A single-component laser Doppler velocimeter was used to measure the inflow velocity. Data were acquired along the 45-deg radial line at two axial locations upstream of the tip path plane ($z/R = -0.04, -0.1$) for steady pitch of 4 and 8 deg, and then with a 4/rev oscillation of 1-deg amplitude superposed on these mean values.

Part II: Unsteady Pressure

The blade surface pressure was measured by Kulite LQ-080-25A absolute pressure transducers as detailed in Ref. 7. Sensors were mounted along chordwise lines at 0.7 and 0.95R on one blade, and at 0.85R on the other blade. Chordwise stations on the upper surface were at x/c of 0.02, 0.05, 0.15, 0.25, 0.35, 0.50, 0.65, and 0.95, and at 0.02, 0.05, 0.15, 0.35, 0.65, 0.95 on the lower surface. Slight variations to this layout occurred at 0.85R where an additional transducer was mounted at $x/c = 0.80$ on the upper surface, and at 0.7R where sensors were mounted on both surfaces at $x/c = 0.07$ instead of 0.05. The transducer layout is detailed in Ref. 7. The test conditions are listed in Table 1.

Correlation Methods

Part I: Inflow Velocity

Inflow velocity has been correlated with Peters' and Su's[8,12] unsteady wake model for rotors. The inflow model, based on an acceleration potential, represents shed vorticity as a three-dimensional skewed cylindrical wake. From the inviscid momentum equation, the inflow can be written as first-order ordinary differential equations (ODEs) in terms of inflow expansion coefficients (state variables). The flowfield and the rotor lift are expanded in terms of appropriate inflow modes, and a set of closed form first-order ODEs in time defines a

finite number of modal inflow states, with blade lift as the forcing function. The modeling lacks wake distortion and roll-up. The blade is a lifting-line blade rotating at Ω rad/s. From the pressure distribution on the actuator disk, average mass flow through the disk, and the influence coefficients between the pressure and inflow (written in terms of the wake skew angle), the inflow expansion coefficients are determined. The generalized forces are determined by spanwise integration of blade sectional lift, which determines induced inflow expansion coefficients. These in turn determine the pressure coefficients (both Φ^V and Φ^Λ) by matrix inversion. The former is related to the induced flowfield by

$$q_i = \frac{1}{U}\int_\xi^\infty \Phi^V_{ri}\, d\xi \tag{1}$$

Part II: Unsteady Pressure

Unsteady pressure has been correlated with Theodorsen's and Loewy's two-dimensional incompressible unsteady aerodynamic theories and with Kaladi's approach of doublet distributions of pulsating strength. These methods are briefly described below.

Theodorsen's Theory

Theodorsen's[10] two-dimensional incompressible aerodynamic theory applies to an infinite wing where the wake lies in the same plane and is shed behind the wing. The method is based on thin airfoil theory and is linear. It does not account for the wake lying underneath the rotor. Thus, the results are insensitive to variations in the lower wake dynamics. The performance of this two-dimensional theory will deteriorate towards the blade tip. For fixed geometry, the unsteady pressure is a function of reduced frequency only. The instantaneous pressure is the sum of the steady and oscillatory pressures due to mean and oscillating pitch, respectively. Equation (2) is the expression for unsteady pressure from Ref. 10. For a simple harmonic pitch oscillation $\theta' = \overline{\theta'}e^{i\omega t}$, the differential pressure loading at any point on the airfoil is $\Delta C_p'(x^*, t) = \overline{\Delta C_p'}(x^*)e^{i\omega t}$. The amplitudes $\overline{\Delta C_p'}$ and $\overline{\theta'}$ are in general complex, including the phase shift between pitch excitation and pressure response. The complex amplitude of the differential unsteady pressure coefficient at a point x^* is

$$\overline{\Delta C_p'}(x^*) = \frac{4}{\pi}\sqrt{\frac{1-x^*}{1+x^*}}\int_{-1}^{1}\sqrt{\frac{1-\xi^*}{1+\xi^*}}\frac{1}{x^*-\xi^*}\frac{\bar{w}(\xi^*)}{U}\,d\xi^*$$
$$+\frac{4}{\pi}[1-C(k)]\sqrt{\frac{1-x^*}{1+x^*}}\int_{-1}^{1}\sqrt{\frac{1-\xi^*}{1+\xi^*}}\frac{\bar{w}(\xi^*)}{U}\,d\xi^*$$
$$-\frac{4ik}{\pi}\int_{-1}^{1}\Lambda(x^*,\xi^*)\frac{\bar{w}(\xi^*)}{U}\,d\xi^* \tag{2}$$

where

$$\Lambda(x^*,\xi^*) = \frac{1}{2}\ln\left(\frac{1-x^*\xi^*+\sqrt{1-x^{*2}}\sqrt{1-\xi^{*2}}}{1-x^*\xi^*-\sqrt{1-x^{*2}}\sqrt{1-\xi^{*2}}}\right)$$

The first two circulatory terms on the right side of Eq. (2) correspond to the contributions of bound vortex and wake vorticity, respectively, and the third term is the apparent mass term due to the inertia of the fluid adjacent to the surface being accelerated. The entire influence of the wake vorticity is contained within this "Theodorsen function." When this equals unity, the wake effect on surface pressure is zero. In terms of Hankel functions, it is

$$C(k) = F(k) + iG(k) = \frac{H_1^{(2)}(k)}{H_1^{(2)}(k) + iH_0^{(2)}(k)} \tag{3}$$

The downwash is obtained from the linearized boundary condition at the surface and is

$$w(x^*) = \bar{w}(x^*)e^{i\omega t} \tag{4}$$

where

$$\frac{\bar{w}(x^*)}{U} = ik\overline{z^*} + \frac{\partial\overline{z^*}}{\partial x^*} \tag{5}$$

and $\overline{z^*}(x^*, t) = -(.5 + x^*)\overline{\theta'}$ for a thin airfoil pitching about quarter-chord $[(x^*)_{c/4} = -0.5]$.

The Cauchy principal value[13] of the integrals in the circulatory terms are evaluated as a limiting process near the integrable singularity. The reduced frequency is calculated first for various operating conditions and radial locations. Theodorsen function values are interpolated from Ref. 14. The apparent mass integral is evaluated numerically. The magnitude and phase of the complex unsteady pressure are extracted.

Loewy's Theory

Loewy's[11] linear, two-dimensional theory includes the wake under the rotor. A trailing vortex sheet extends to infinity aft of the trailing edge and several layers of planar wake vortex sheets lie underneath, extending to infinity on either side of the blade section. The effects of wake dynamics on unsteady loads are captured, but finite-span effects are not captured. The trailing vortices shed from other sections of the rotor do not affect the unsteady loading at the radial location of interest. Thus, significant error is expected near the blade tip. The theory developed in Ref. 11 becomes identical to Theodorsen's theory if the Theodorsen function of Eq. (3) is replaced by the modified lift deficiency function $[C'(k, n, h) = F' + iG']$ given by Eq. 6:

$$C'(k,n,h) = \frac{H_1^{(2)}(k) + 2J_1(k)W(kh,n)}{H_1^{(2)}(k) + iH_0^{(2)} + 2[J_1(k) + iJ_0(k)]W(kh,n)} \tag{6}$$

where

$$H_0^{(2)}(k) = J_0(k) - iY_0(k) \tag{7}$$

$$H_1^{(2)}(k) = J_1(k) - iY_1(k) \tag{8}$$

The wake weighting function for a two-bladed rotor for collective pitch oscillation, $W(kh, n)$ is given by Eq. 9:

$$W(kh,n) = \frac{1}{e^{kh}e^{i\pi n} - 1} \tag{9}$$

The Bessel functions $J_0(k)$, $J_1(k)$, $Y_0(k)$, and $Y_1(k)$ are obtained from Ref. 15. $C'(k, n, h)$ is calculated and $C(k)$ in Theodorsen's theory is replaced by C'. As the wake spacing h increases, the effects of wake vortex sheets lying under the rotor diminish and Theodorsen's results are obtained in the limit as $h \to \infty$, when $C'(k, n, h) \to C(k)$. Thus, Theodorsen's theory is a special case of Loewy's development. Loewy's method is applicable to nonzero, low inflow cases; the theory breaks down for zero inflow velocity corresponding to the zero mean pitch case for a symmetrical airfoil section.

Kaladi's Method

Kaladi's[9] used an incompressible doublet distribution with harmonically pulsating strength on the rotor and in the wake. Unsteady pressure loading is obtained by differentiating the doublet strength. The panel method models the blade surface doublet strength with chordwise and spanwise control panels.

whereas the modal method represents the surface doublet strength by a series of chordwise and spanwise functions. The wake is modeled by panels in both cases. The modal method differs from the panel method only in the use of a continuous (as opposed to discrete) doublet distribution on the blade surface. The distribution shape is determined by experience with the shape of the pressure distribution. The doublet strength gradient is assumed to be infinite at the leading edge and zero at the trailing edge. A Legendre polynomial expansion is used for the spanwise distribution. A Maclaurin series expansion in terms of reduced frequency is used to evaluate integrals for unit reduced frequency at the blade tip (Ref. 9, p. 103). Once the integrals over the blades are obtained, influence coefficients are determined by interpolation for a specified frequency. Multhopp's distribution of collocation points is used and the number of modes is made exactly equal to the number of collocation points.

Kaladi's methods as used in this article used 2 spanwise and 5 chordwise panels to represent the rotor surface for the panel method. Five spanwise and 2 chordwise modes were chosen for the modal method. The wake was truncated after 5 revolutions, and 180 panels were used in both cases with an azimuthal width of 10 deg.

Results and Discussion

Part I: Inflow Velocity

Steady Pitch Inflow Velocity

Figure 1 shows the radial variation of the time-averaged inflow velocity (normalized using tip speed) at $z/R = -0.04$ for steady pitch of 4 deg. Agreement between the experiment and Peters' modal theory[8] is excellent in the inboard region. Large deviations in the tip region are attributed to the inability of the lifting line analysis to capture the tip vortex roll-up. Figure 2 shows the azimuthal variation of inflow velocity at $r/R = 0.824$ at a steady collective pitch of 4 deg. The result agrees well with the analytical prediction, except for underprediction of the extrema at blade passage, which is attributed to the truncation of the analytical model at 24 harmonics as stated in Ref. 8.

Oscillatory Pitch Inflow Velocity

Figure 3 shows the comparison between Peters' analysis[8] and experiments at $r/R = 0.765$ for 4/rev pitch oscillation. Again, the inflow extrema during the blade passage interval are underpredicted. The time history of raw data was examined to ensure that averaging was sufficient to yield reliable results. Again, good correlation of unsteady inflow with analytical prediction has been obtained.

Part II: Unsteady Pressure

Figures 4 and 5 show amplitude and phase angle of unsteady perturbation pressure at 70% radial location for various har-

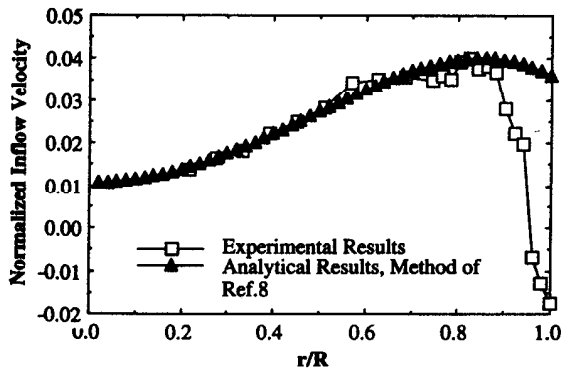

Fig. 1 Radial distribution of averaged normalized inflow velocity at $z/R = -0.04$ for steady pitch of 4 deg, compared with results from Su and Peters.[8]

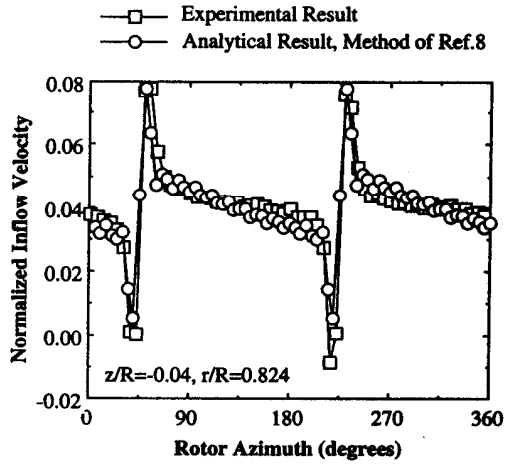

Fig. 2 Azimuthal variation of inflow velocity at $r/R = 0.824$ for steady pitch of 4 deg, compared with results from Su and Peters.[8]

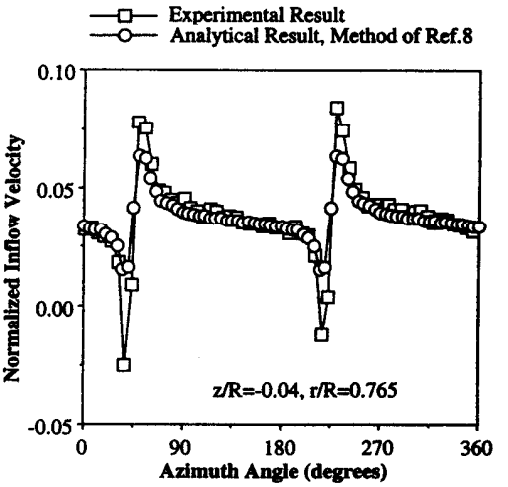

Fig. 3 Azimuthal inflow velocity variation at $r/R = 0.765$ for 4/rev pitch oscillation about $\theta_0 = 4$ deg, compared with results from Su and Peters.[8]

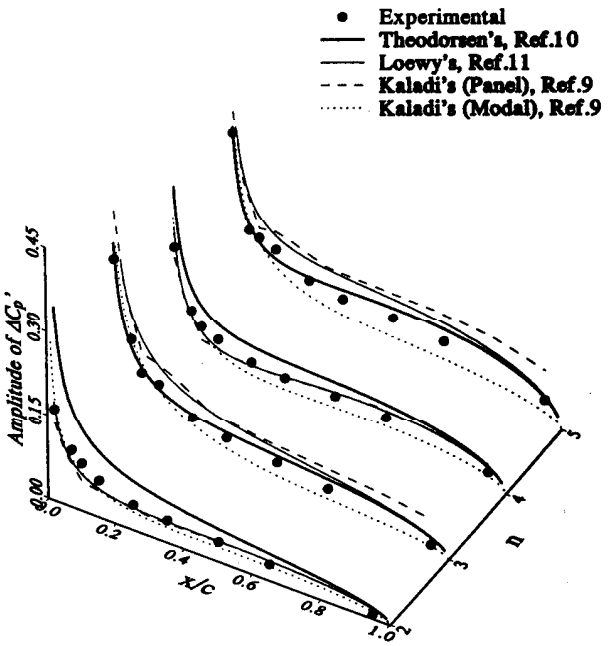

Fig. 4 Lifting perturbation pressure amplitude at 0.70*R*.

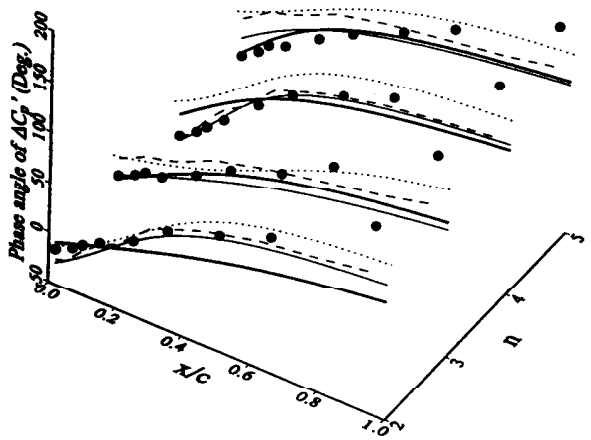

Fig. 5 Lifting perturbation pressure phase angle at 0.70*R*.

monics of forcing frequency n. As described in Ref. 7, the test conditions given in Table 1 should be divided into two groups for studying wake dynamics effects depending on even or odd values of the harmonics of forcing frequency n. Analytical and numerical methods (except Theodorsen's method) are also sensitive to this phase effect. These two groups are therefore dealt with separately. It is also useful to divide test conditions along the radius into inboard and outboard stations for analyzing the results. The former have a small spanwise gradient of bound circulation and, hence, resemble the two-dimensional case, while the latter require three-dimensional analyses. Also, the effects of reduced frequency can be seen in two ways: 1) by varying n at a fixed r/R or 2) by changing r/R at fixed n. Different figures must be compared for the latter case.

Phase Effects

At all radial locations Theodorsen's theory predicts higher unsteady pressure amplitude for even harmonics of forcing frequency. Since Theodorsen's theory does not account for vorticity in the rotor wake, it is not able to capture the phase effects described in Refs. 6 and 7. Due to the 180-deg phase shift between successive layers of wake vorticity, the vorticity in the wake tends to cancel out for odd harmonics of forcing frequency and a jump in pressure amplitude is recorded during measurement for these cases. Theodorsen's theory only experiences a change in the reduced frequency and predicts a small change in pressure. Therefore, when n is increased from 2 to 3 or from 4 to 5, the theory predicts a small increase in pressure amplitude while the experiment records a large increase, eliminating large discrepancies between the theory and experiment at even harmonics of forcing frequency and bringing them closer at odd harmonics. The discrepancies increase outboard because the theory does not account for tip effects.

Inboard Location: Reduced Frequency Effects

At sufficiently inboard radial locations for even harmonics of forcing frequencies (see Figs. 4 and 5, n = 2, 4), Theodorsen's method overpredicts the amplitude, as expected, and also fails to capture the slope of the chordwise phase distribution profile. As frequency increases, correlation with Theodorsen's method seems to improve both in amplitude and phase. The effects of wake vorticity on blade unsteady loading diminish with increasing frequency for even harmonics of forcing frequency. Therefore, Theodorsen's theory is expected to correlate better at very high frequency. Kaladi's modal method consistently underpredicts the amplitude and overpredicts the phase; the correlation becomes worse at high frequency. Loewy's theory and Kaladi's panel method converge to each other both in amplitude and phase of the unsteady perturbation pressure, though only 10 panels (2 spanwise and 5 chordwise) have been used in Kaladi's panel method. More chordwise panels are needed to obtain a smooth curve for amplitude distribution. The convergence of the area under experimental and analytical amplitude of $\Delta C_p'$ curves increases with forcing frequency. It therefore appears that these two methods predict better at higher frequency. The analytical unsteady perturbation pressure amplitude and phase profiles also tend to converge to the data (see Figs. 4 and 5, n = 4) with increasing frequency. The discrepancy in profile shapes can be attributed to the effects of rotation or possibly the viscous effects.

Effects of Rotational Speed

As frequency increases, the reduced frequency increases proportionately. The effect of rotational speed is lower at higher reduced frequency. Effects of rotation should be observed at low frequency as underprediction of both amplitude and phase near the leading edge, and overprediction of amplitude aft of midchord. If rotation is neglected, prediction of amplitude and phase improves with frequency. Prediction of phase is excellent except for the problems near the trailing edge that are discussed later. As k is increased, the phase profile rotates and steepens as expected. The steep chordwise phase variation for n = 4 is predicted closely by both Loewy's theory and Kaladi's panel method (Fig. 5). Loewy's theory thus provides an inexpensive tool for predicting amplitude and phase of unsteady pressure at sufficiently inboard radial location for even harmonics of forcing frequency, especially at high frequency. Viscous effects are not accounted for in any of the analyses. A better prediction of chordwise amplitude and phase distribution profile shapes is expected if these effects are included.

Inboard Location: Odd Harmonics

At sufficiently inboard radial locations for odd harmonics of forcing frequency, Loewy's theory predicts higher pressure amplitude because the wake model includes phase effects as discussed earlier (Fig. 4). In fact, the wake does not contribute much and the pressure amplitude does not increase to the extent predicted by the theory. The correlation worsens with increasing frequency. In these cases, a discrepancy exists between Loewy's theory and Kaladi's panel method and increases with reduced frequency. Remarkable discrepancies exist between the phase distribution profiles of these two methods. Kaladi's modal method still consistently underpredicts the amplitude and overpredicts the phase, the correlation worsening with increasing frequency. Theodorsen's theory, on the other hand, comes surprisingly close to the data at low frequency. The correlation, however, unlike the case of even harmonics, starts worsening with increasing frequency. It therefore appears that the wake vorticity layers tend to annul each other for odd harmonics of forcing frequency at low frequency. The phase distribution profile in any case is closer to the experimental data as compared to the other three methods. Theodorsen's theory thus provides a very efficient tool for predicting amplitude and phase of unsteady pressure at sufficiently inboard radial location for odd harmonics of forcing frequency, especially at low frequency.

Outboard Location: Even Harmonics

Figures 6 and 7 show amplitude and phase of unsteady perturbation pressure at 0.85*R* for various harmonics of forcing frequency n. Similarly, Figs. 8 and 9 show amplitude and phase of unsteady perturbation pressure at 0.95*R* for various harmonics of forcing frequency n. As we move outboard, the above trends change completely. At outboard radial locations for even n (see Figs. 8 and 9, n = 2, 4), Theodorsen's predictions of amplitude are much larger than the experimental data, because the theory is two dimensional. The phase profile predictions are also flatter than the experiment. Although the amplitude decreases and the phase profile slightly steepens

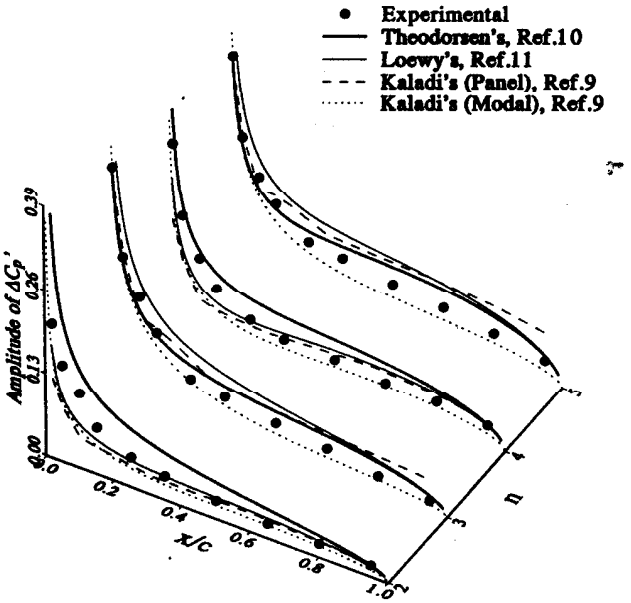

Fig. 6 Lifting perturbation pressure amplitude at 0.85*R*.

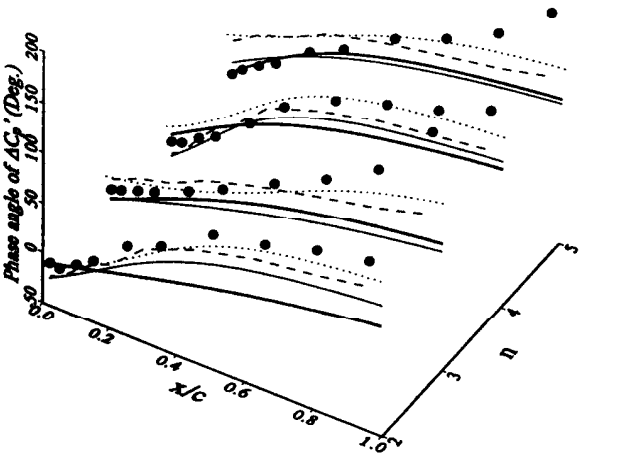

Fig. 7 Lifting perturbation pressure phase angle at 0.85*R*.

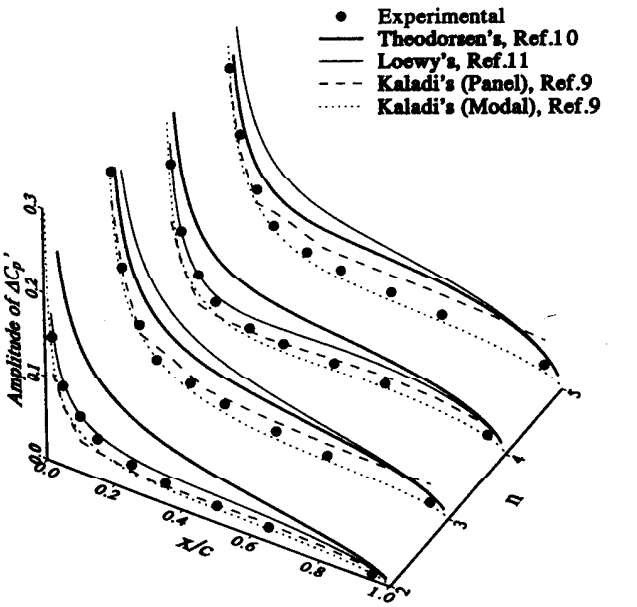

Fig. 8 Lifting perturbation pressure amplitude at 0.95*R*.

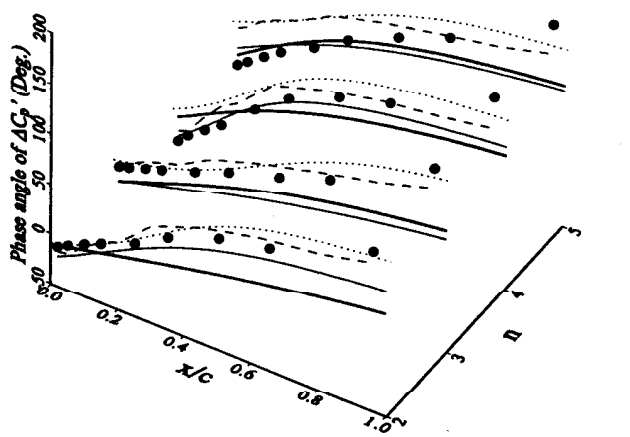

Fig. 9 Lifting perturbation pressure phase angle at 0.95*R*.

with increasing frequency, they still differ from experimental data even at high frequency. Loewy's two-dimensional theory also overpredicts the amplitude over the entire chord except in the leading-edge region. The correlation worsens with increasing frequency. Now, substantial discrepancies exist between Loewy's theory and Kaladi's panel method, mainly due to the latter's capability of modeling tip effects. Kaladi's panel method comes close to the modal method at low frequency, but starts departing from it for high frequency. With increasing frequency the modal method comes closer to the experimental data, and with increasingly high frequency the correlation is expected to improve. At high frequency, good correlation of the phase distribution profile has been obtained with Loewy's theory (Fig. 9, $n = 4$). At low frequency, the modal method comes close to the experimental phase data.

Outboard Location: Odd Harmonics

At outboard radial locations for odd harmonics of forcing frequencies, Loewy's theory still predicts higher pressure amplitude because of the phase effects as discussed earlier, and three-dimensional effects. The correlation worsens with increasing frequency. A large discrepancy exists between Loewy's theory and Kaladi's panel method and increases with reduced frequency mainly due to the latter's capability of modeling tip effects. The latter comes closer to the experimental data. Once again, substantial discrepancies exist between phase distribution profiles of these two methods. Although the panel method comes close to the experiment, it slightly overpredicts the amplitude. The correlation worsens with increasing frequency. The modal method correlates the amplitude of unsteady pressure very well at low frequency, but slightly underpredicts at high frequency. The panel method phase approaches that of the modal method at all frequencies. These two methods correlate phase well at low frequency, but overpredict at high frequency. At high frequency, like the case of inboard radial location, Theodorsen's theory correlates the phase better. The choice of methods that correlate well with the data at different radial location and test conditions can be made from Table 2.

Inboard Location: Mean Pitch Effects

Figures 10 and 11 show amplitude and phase angle of unsteady perturbation pressure correlation graphs at $\omega = 40$ Hz, $\Omega = 10$ Hz, $n = 4$ for various mean pitch angle θ_0 at 0.70*R*. As discussed earlier, Kaladi's panel method follows Loewy's theory closely and correlates well with the experiment for even harmonics of forcing frequency at sufficiently inboard radial locations. When mean pitch is increased, the correlation deteriorates. The inflow velocity and, hence, the wake spacing increase with mean pitch. The effect of wake vorticity reduces and recovery in unsteady pressure is expected. Thus, as expected, theory predicts higher amplitude

Table 2 Methods that correlate well with experimental data

	Even n				Odd n			
	Low frequency		High frequency		Low frequency		High frequency	
Location	Amp	Phase	Amp	Phase	Amp	Phase	Amp	Phase
Inboard	B,C	B,C	B,C	B,C	A	A	A	A
Outboard	C	D	D	B	D	C,D	D	A

Key: A, Theodorsen's theory; B, Loewy's theory; C, Kaladi's panel method; and D, Kaladi's modal method.

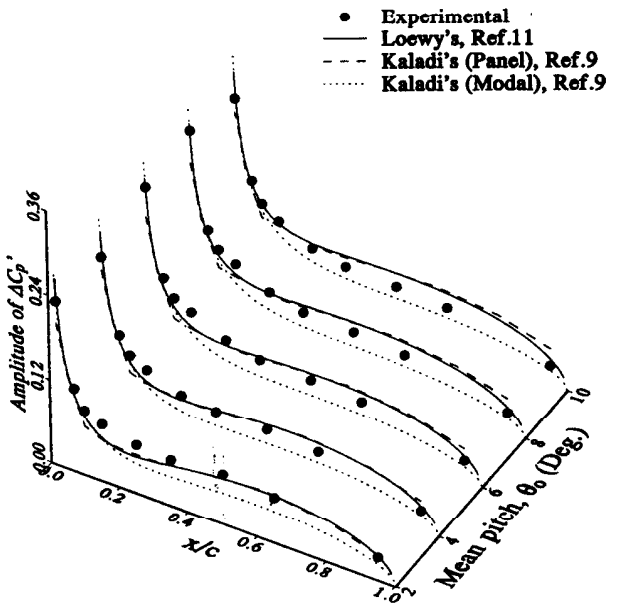

Fig. 10 $\Delta C_p'$ amplitude at 0.70R for various mean pitch angles.

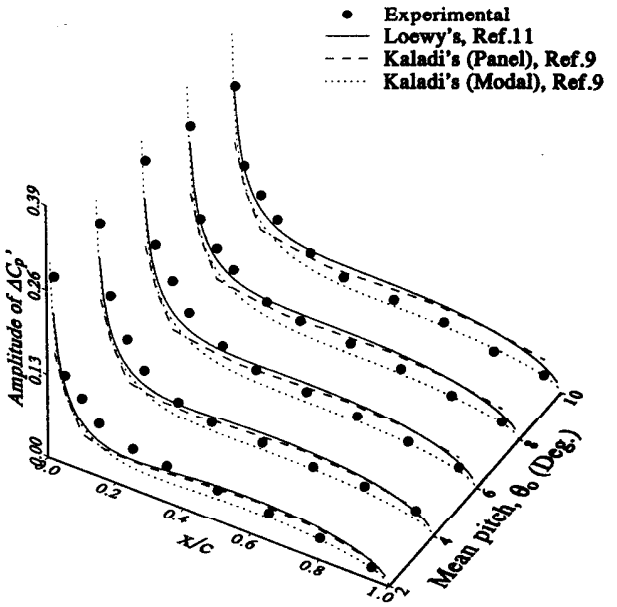

Fig. 12 $\Delta C_p'$ amplitude at 0.85R for various mean pitch angles.

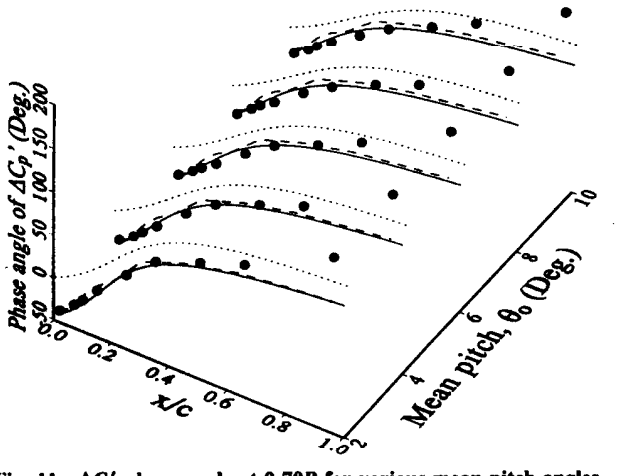

Fig. 11 $\Delta C_p'$ phase angle at 0.70R for various mean pitch angles.

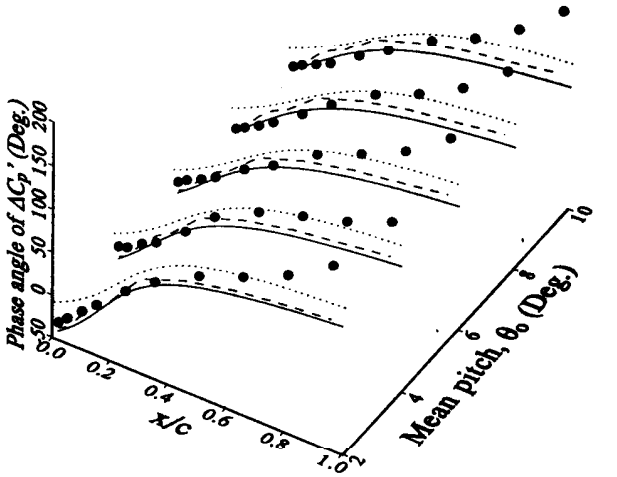

Fig. 13 $\Delta C_p'$ phase angle at 0.85R for various mean pitch angles.

at high mean pitch. The experimental amplitude first increases with mean pitch and then falls. At low inflow, Loewy's theory and panel method correlate well in the leading- and trailing-edge regions, but underpredict amplitude in the midchord region. With increasing inflow, these two methods diverge from each other and rapidly from the data. Analytical predictions are higher than the experiment all along the chord except near the leading edge. Kaladi's modal method consistently underpredicts amplitude and overpredicts phase at all inflow conditions at an inboard radial location. The phase is predicted very well by Loewy's theory and panel method at low inflow, and by Loewy's theory at even high inflow. The panel method phase diverges from Loewy's theory and the experiment with increasing inflow. Perhaps more chordwise and spanwise panels are required for better correlation.

Outboard Location: Mean Pitch Effects

Figures 12 and 13 show amplitude and phase of unsteady perturbation pressure for various θ_0 at 0.85R. Figures. 14 and 15 show amplitude and phase of unsteady perturbation pressure for various θ_0 at 0.95R. As we move outboard, the trends change significantly. A significant discrepancy appears between Loewy's theory and the panel method due to three-dimensional effects (Figs. 14 and 15). This discrepancy increases with θ_0 as expected. Loewy's predictions are now higher than panel method predictions. At very low inflow, Loewy's method correlates well with the experiment. Kaladi's modal method underpredicts amplitude at very low inflow. For moderate inflow, the panel method correlates better. At high inflow, excellent correlation is obtained with the modal method.

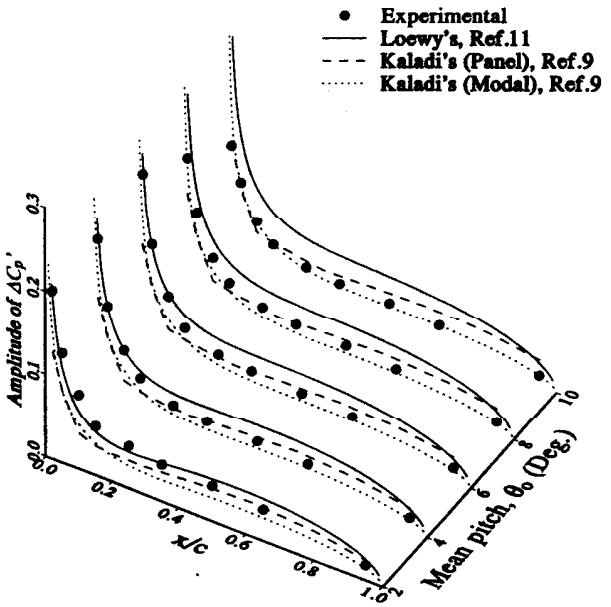

Fig. 14 $\Delta C_p'$ amplitude at 0.95R for various mean pitch angles.

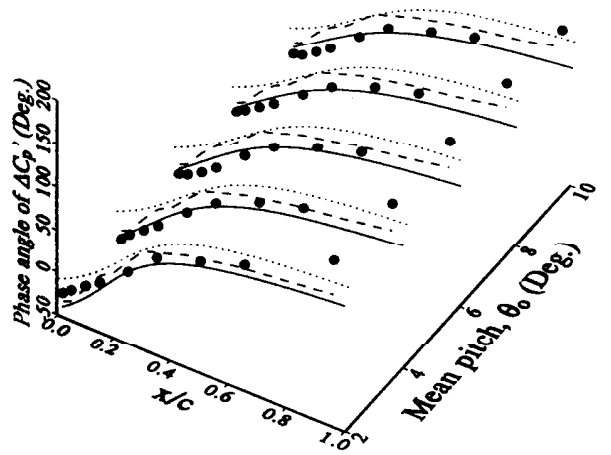

Fig. 15 $\Delta C_p'$ phase angle at 0.95R for various mean pitch angles.

A discrepancy in phase exists between Loewy's theory and panel method, increasing with θ_0. At very low inflow, the panel method correlates phase better. Loewy's method correlates phase better with increasing inflow, and can thus be used for predicting phase even at an outboard location.

Discrepancy in Phase Correlation

In all cases, a poor correlation of phase is obtained near the trailing edge. This may be because all of the predictions extract phase from a complex representation of unsteady pressure. Near the trailing edge, the pressure amplitude approaches zero to satisfy the Kutta condition, and hence, in extracting phase from complex unsteady pressure, division by a small quantity amplifies the error. Therefore, the phase near the trailing edge is not reliable. In the experiments, the time history of pressure is recorded and a curve-fitting technique is employed. The phase is extracted as that needed to match a standard sinusoidal waveform to the recorded pressure time history. Therefore, the experimental phase angle is more accurate.

Conclusions

Measurements of inflow velocity and chordwise pressure variations on a two-bladed full-scale teetering tail rotor in hover have been correlated with analytical predictions, with and without dynamic pitch excitation. The conclusions are as follows:

Part I: Inflow Velocity

1) The spanwise variation of the inflow velocity is predicted very well by Peters' modal theory, except near the tip. As expected, the measured inflow velocity drops towards the tip.

2) Both steady and oscillatory inflow velocity data agree with Peters' theory. The theory underpredicts the extrema of inflow velocity variation due to blade passage.

3) The inflow response to pitch perturbation decreases in amplitude near the blade tip.

Part II: Unsteady Pressure

1) The different features of the various prediction methods result in good correlations at different test conditions and locations, as summarized in Table 2.

2) At inboard radial locations, Loewy's theory and Kaladi's panel method converge and correlate well in both amplitude and phase of unsteady perturbation pressure for even harmonics of forcing frequency.

3) Theodorsen's theory comes surprisingly close to the experimental data at an inboard radial location at low frequency for odd n. Thus, at inboard locations, the linear two-dimensional theories serve as inexpensive but reliable tools for predicting unsteady pressure over the rotor blade. Kaladi's modal method consistently underpredicts the amplitude and overpredicts the phase at an inboard radial location.

4) At outboard radial locations, Kaladi's panel method works best for low frequency and the modal method for high frequency for even n for predicting amplitude. For the phase, the modal method works best for low frequency and Loewy's theory for high frequency for even n. For odd n, the modal method should be used for amplitude and phase at low frequency. The Modal method should be used for amplitude and Theodorsen's method for phase at high frequency. These conclusions are summarized in Table 2.

5) When mean pitch angle is increased, the correlation with Kaladi's panel method and Loewy's theory deteriorates. The phase is predicted very well by Loewy's theory and the panel method at low inflow, and by Loewy's theory at high inflow.

6) At an outboard radial location, Loewy's theory should be used at low inflow and the panel method at moderate inflow. At high inflow, excellent correlation is obtained with the modal method. For phase, the panel method should be used at low inflow and Loewy's theory for increasing inflow.

7) A discrepancy exists in phase near the trailing edge for all cases. The experimental phase angle is more reliable.

Acknowledgments

This work was supported by the U.S. Army Research Office, under Aeroelasticity Task 3 of the Center of Excellence in Rotary Wing Aircraft Technology, Thomas L. Doligalski is the Technical Monitor.

References

[1]Satyanarayana, B., and Davis, S., "Experimental Studies of Unsteady Trailing-Edge Conditions," *AIAA Journal*, Vol. 16, No. 2, 1978, pp. 125–129.

[2]Ardonceau, P. L., "Unsteady Pressure Distribution over a Pitching Airfoil," *AIAA Journal*, Vol. 27, No. 5, 1989, pp. 660–662.

[3]Basu, B., and Hancock, G., "The Unsteady Motion of a Two-Dimensional airfoil in Incompressible Inviscid Flow," *Journal of Fluid Mechanics*, Vol. 87, Pt. 1, 1978, pp. 159–178.

[4]Commerford, G. L., and Carta, F. O., "Unsteady Aerodynamic Response of a Two-Dimensional Airfoil at High Reduced Frequency," *AIAA Journal*, Vol. 12, No. 1, 1974, pp. 43–48.

[5]Lorber, P. F., and Covert, E. E., "Unsteady Airfoil Pressures Produced by Periodic Aerodynamic Interference," *AIAA Journal*, Vol. 20, No. 9, 1982, pp. 1153–1159.

[6]Liou, S. G., Komerath, N. M., and Lal, M. K., "Measurements Around a Rotor Blade Excited in Pitch, Part 1: Dynamic Inflow,"

Journal of the American Helicopter Society, Vol. 39, No. 2, 1994, pp. 3–12.

[7]Lal, M. K., Liou, S. G., Pierce, G. A., and Komerath, N. M., "Measurement Around a Rotor Blade Excited in Pitch, Part 2: Unsteady Surface Pressure," *Journal of the American Helicopter Society*, Vol. 39, No. 2, 1994, pp. 13–20.

[8]Su, A., Yoo, K. M., and Peters, D. A.,"Extension and Validation of an Unsteady Wake Model for Rotors," *Journal of Aircraft*, Vol. 29, No. 3, 1992, pp. 374–383.

[9]Kaladi, V. M., "Unsteady Compressible Lifting Surface Analysis for Rotary Wings Using Velocity Potential Modes," Ph.D. Dissertation, School of Aerospace Engineering, Georgia Inst. of Technology, Atlanta, GA, Aug. 1990.

[10]Theodorsen, T., "General Theory of Aerodynamic Instability and the Mechanism of Flutter," NACA Rept. 496, 1935.

[11]Loewy, R. G., "A Two-Dimensional Approximation to the Unsteady Aerodynamics of Rotary Wings," *Journal of the Aeronautical Sciences*, Vol. 24, No. 2, 1957, pp. 81–92.

[12]Peters, D. A., Boyd, D. D., and He, C. J.,"Finite-State Induced-Flow Model for Rotors in Hover and Forward Flight," *Journal of the American Helicopter Society*, Vol. 34, No. 4, 1989, pp. 5–17.

[13]Korn, G. A., and Korn, T. M., *Mathematical Handbook for Scientists and Engineers*, McGraw–Hill, New York, 1961.

[14]Van de Vooren, A. I., "Collected Tables and Graphs," *Manual on Aeroelasticity*, Vol. VI, NATO, Advisory Group for Aeronautical Research and Development, Oct. 1968.

[15]Watson, G. N., *Theory of Bessel Functions*, Cambridge Univ. Press, Cambridge, England, UK, 1944, pp. 666–697.